Published in final edited form as:
*J Pharm Sci*. 2014 May ; 103(5): 1478–1486. doi:10.1002/jps.23921.

# Hydrogel-forming microneedles increase in volume during swelling in skin, but skin barrier function recovery is unaffected

**Ryan F. Donnelly***, **Karen Mooney**, **Maelíosa T.C. McCrudden**, **Eva M. Vicente-Pérez**, **Luc Belaid**, **Patricia González-Vázquez**, **James C. McElnay**, and **A. David Woolfson**
School of Pharmacy, Queen's University, Belfast, 97 Lisburn Road, Belfast, BT9 7BL, UK

## Abstract

We describe, for the first time, quantification of in-skin swelling and fluid uptake by hydrogel-forming microneedle arrays (MN) and skin barrier recovery in human volunteers. Such MN, prepared from aqueous blends of hydrolysed poly(methylvinylether/maleicanhydride) (15% w/w) and the crosslinker poly(ethyleneglycol) 10,000 daltons (7.5% w/w), were inserted into the skin of human volunteers (n = 15) to depths of approximately 300 μm by gentle hand pressure. The MN swelled in skin, taking up skin interstitial fluid, such that their mass had increased by approximately 30% after 6 hours in skin. Importantly, however, skin barrier function recovered within 24 hours post microneedle removal, regardless of how long the MN had been in skin or how much their volume had increased with swelling. Further research on closure of MN-induced micropores is required, since transepidermal water loss measurements suggested micropore closure, while optical coherence tomography indicated that MN-induced micropores had not closed over, even 24 hours after MN had been removed. There were no complaints of skin reactions, adverse events or strong views against MN use by any of the volunteers. Only some minor erythema was noted after patch removal, although this always resolved within 48 hours and no adverse events were present on follow-up.

### Keywords

Microneedle; hydrogel; micropore; skin barrier

## Introduction

Microneedle (MN) arrays are minimally-invasive devices that painlessly, and without causing bleeding, penetrate the skin to enhance intradermal and transdermal drug delivery.[1,2] MN devices are not equivalent to conventional transdermal patches, in that they are not simply applied to the skin surface. Rather MN function principally by breaching the skin's protective *stratum corneum* barrier and often penetrate into the viable epidermis and dermis.[1,3] Such areas of the body are normally sterile. Accordingly, it is imperative that MN do not contain microbial loads sufficient to cause skin or systemic infection or stimulate the

*Corresponding author: Dr. Ryan F. Donnelly, Reader in Pharmaceutics, School of Pharmacy, Queen's University Belfast, Medical Biology Centre, 97 Lisburn Road, Belfast, BT9 7BL, UK, Tel: +44 (0) 28 90 972 251, Fax: +44 (0) 28 90 247 794, r.donnelly@qub.ac.uk.

**Conflict of interest statement:** We have no personal, financial or non-financial conflicts of interest.


Europe PMC Funders Author Manuscripts

immune system. In addition, since the *stratum corneum* protects against chemical and particulate ingress as well as that of microorganisms, it is essential that its barrier function is rapidly restored following MN removal.

MN-based approaches to sustained drug delivery often involve puncturing the *stratum corneum* using solid silicon, metal or polymeric MN, followed by occlusion of a drug-containing gel or patch, with the resulting over-hydration of the skin keeping micropores open for up to 48 hours.[4,5] Non-steroidal anti inflammatory drugs and statins have also been used to prolong micropore lifetime for up to 7 days post MN removal.[6,8] Modulating pH does not seem to affect micropore closure kinetics significantly.[9] As an alternative to these two-step "poke and patch" approaches, we developed hydrogel-forming MN arrays that contain no drug themselves.[10-12] Instead, they rapidly imbibe skin interstitial fluid upon insertion to form continuous, unblockable conduits between the dermal microcirculation and an attached patch-type drug reservoir (Figure 1A). These systems, which are held in place using an adhesive backing layer, are intended to improve patient convenience through their one-step method of application. Sustained administration of peptides, proteins and small water soluble drugs is facilitated by the swollen hydrogel MN, which keep the micropores open until removal. Such MN were found to be free from microorganisms and to exhibit active antimicrobial properties[11]. We have recently shown that human volunteers can reproducibly insert these MN by hand, once given appropriate written instructions and when counselled by a pharmacist.[13] Since the mechanism of action of these MN involves an increase in volume during skin residence, it is important to determine the effects of this on skin barrier recovery. Accordingly we have, for the first time, studied the influence of insertion time on MN dimensional changes, micropore morphology and restoration of skin barrier integrity in human volunteers.

## Materials and Methods

### Chemicals

Polyethylene glycol (PEG, MW 10,000 Da) was purchased from Sigma-Aldrich, Dorset, UK. Gantrez® AN-139, a copolymer of methyl vinyl ether and maleic anhydride (PMVE/MAH), was a gift from Ashland, Kidderminster, UK. All other chemicals used were of analytical reagent grade.

### Fabrication of hydrogel-forming MN arrays

Aqueous blends containing 15% w/w Gantrez® AN139 and 7.5% w/w PEG, 10,000 were utilized to fabricate MN arrays, as previously described.[10,11] The blend (500 mg) was poured into MN moulds (361 (19×19) needles perpendicular to the base and of conical shape, 600 μm high with base width of 300 μm and 50 μm interspacing on a 0.49 $cm^2$ patch) and these were centrifuged at 3000 g for 15 min and dried at room temperature for 48 h. MN were crosslinked (esterification reaction) by heating at 80°C for 24 hours and the sidewalls formed by the moulding process were removed using a heated blade (Figure 1B).[10,11,14,15]

### Patch preparation

Following the removal of the side walls, patches were created by attaching the MN arrays to Sellotape® immediately prior to application. This method of adhesion was selected to facilitate the use of optical coherence tomographic imaging, as detailed below. The MN-free patches were produced according to the same procedure, but instead involved the use of a baseplate mould, rather than the MN mould, to form MN baseplates with no needles.

### Volunteers

Following local ethical committee approval, healthy human volunteers were recruited to take part and those with any prior dermatological conditions excluded from the study. Recruitment was by convenience sampling of postgraduate students within the School of Pharmacy. Students were provided with an information sheet, providing a clear outline of the study, and a consent form to be returned if willing to participate. This consent form was also used as a screening tool to ensure the exclusion criteria were adhered to. Participants were asked to avoid the application of cosmetics to the forearms during the study and for 24 hours prior to its commencement. The forearms were also to remain uncovered with garments and protected from moisture during the time of the study.

### Study protocol

The study was undertaken in a temperature controlled environment, maintained at 20°C, within the School of Pharmacy, Queen's University Belfast. Volunteers (n = 15) rested within the room with their ventral forearms uncovered for at least 15 minutes prior to the study and for at least 15 minutes prior to each measurement during the study.[16] Six different locations (three per arm) were then outlined on the forearms of each volunteer using a marker, enabling the clear identification of each patch area (Figure 2A). MN and MN-free patches (baseplates) were then applied by a single operator to each of these six sites using gentle thumb pressure for approximately 10 seconds. Volunteers were not informed as to which patches contained MNs and which did not. The time of each application was carefully recorded and, at various time points, each patch was removed, as outlined in Table 1A.

### MN mass change

The mass of each MN array was recorded at the outset using an analytical balance (APX-60, Denver Instrument, New York, USA). This was repeated immediately after removal from each volunteer, following the detachment of the MN array from the Sellotape® backing. An estimation of fluid uptake could then be recorded for each time period of patch application for each volunteer and the percentage mass change calculated.

### Optical coherence tomography

Optical coherence tomography (OCT) was used in this study for two purposes: firstly, to follow the behaviour of the MN arrays in real-time while *in situ* for each volunteer and, secondly, to monitor the recovery of skin after removal of MN arrays. OCT is a non-invasive optical imaging technique that is analogous to ultrasound, whereby OCT maps the variation of reflected light, rather than sound, from a biological sample as a function of depth.[17] Due to extensive light scattering by tissue, the typical penetration depth of

conventional optical techniques is low. OCT, however, is capable of penetrating skin to depths of approximately 2.0 mm, in comparison to confocal microscopy, which can only reach depths of around 0.25 mm.[18] OCT, therefore, is the only optical method suitable for non-invasive cross-sectional imaging of the epidermis and upper dermis *in vivo*. It is, accordingly, a valuable method for monitoring MN dimensional changes in skin and micropore morphology and we have made extensive use of OCT in previous *in vitro* and *in vivo* studies.[10,19,20]

Only the arrays in place for the entire 6 hour study period were examined for each volunteer, i.e. the patch located at application site 1 (Figure 2A). OCT scans (VivoSight™ Topical Multi-Beam OCT Handheld Probe, Michelson Diagnostics Ltd, Kent, UK) were taken immediately following patch application (t = 0) and again at t = 0.5, 1, 2, 4 and 6 hours after insertion. The resultant images were then exported to ImageJ® (National Institutes of Health, Bethesda, MD, USA) and measurements of MN height and base diameter recorded for each time point. For each volunteer, a total of 36 individual MNs were measured per time point and the mean (± S.D.) MN height and base diameters recorded. MN volume was also calculated based on their conical shape.

OCT scans of the skin following the different periods of MN residence were taken immediately following MN removal (t = 0) and at 3 hours and 24 hours. The resultant images were then analysed to provide an indication of skin recovery. Using ImageJ®, each scan was transformed to construct an approximation of a microscope view of the skin surface (aerial perspective). In each case, this image was then inspected for a visible line of pores caused by MN penetration. This line could then be examined in greater detail, by transposing this selected area back into the 2d side-on-view and measurements taken (μm) of pore depth (d) at the skin surface and width (w), as shown in Figure 2B. In each case, measurements were taken for 25 visible pores and the mean (± S.D.) depth and width (μm) calculated. For each volunteer and each MN residence time the mean (± S.D.) pore depth and width (μm) were separately plotted against time (hr), such that an area under the curve (AUC) value (μm.hr) could be obtained in each case relating to depth ($AUC_{depth}$) and width ($AUC_{width}$).

## Transepidermal water loss measurement

Transepidermal water loss (TEWL) measurements were obtained using a VapoMeter® (Delfin Technologies Ltd, Kuopio, Finland). This is a closed chamber device which is capable of measurements of water loss up to 300 $g/m^2hr$. The TEWL values were obtained by placing the meter on the relevant area, ensuring the skin was sealed by the adapter. The mean (± S.D.) baseline TEWL ($g/m^2hr$) was measured for each volunteer prior to patch application. TEWL was then measured immediately after patch removal at each site (t = 0) and again at the subsequent time points of t = 0.5, 0.75, 1, 2, 3, and 24 hr.

## Clinical questionnaire

A questionnaire was used to assess pain and sensation, allow opportunity for further comment and record participant demographics. To assess pain and sensation, the questionnaire included the Short-Form McGill Pain Questionnaire (SF-MPQ). This is a

three-part tool based on a Pain Rating Index (PRI), Present Pain Intensity (PPI) and a VAS.[21] The SF-MPQ was used to measure pain and sensation on three separate instances in this study, as specified in Table 1B.

The PRI consisted of 15 pain descriptors and were each rated as follows; 0 = none, 1 = mild, 2 = moderate and 3 = severe. The initial 11 descriptors related to sensory pain while the remaining terms were associated with affective pain, thus enabling the generation of a sensory score, affective score and total score in each case. PPI was measured using the 6-point scale of 0 = no pain, 1 = mild, 2 = discomforting, 3 = distressing, 4 = horrible and 5 = excruciating. The VAS used was a 10 cm line ranging from 'No pain' (0 cm) to 'Worst pain possible' (10 cm). The questionnaire was also used to ascertain if participants found application different at different application sites and included space for additional comments. These comments were then transcribed verbatim and the main themes noted.

### Statistical analysis

Analysis was performed using a number of statistical tests, as appropriate, including the Kruskal Wallis Test, Mann-Whitney U test, Wilcoxan-signed rank, Paired t-test, one-way between groups ANOVA with Tukey HSD test, Friedman Test and Chi-squared test. In all cases, $p < 0.05$ denoted significance.

## Results

### Demographics

A total of 15 volunteers (8 male) were recruited to the study. These participants had a mean (± S.D.) age of 30 (± 7.43) years and were of various ethnicities (Northern Ireland Statistics and Research Agency, 2013), as shown in Table 1C. Those who selected 'Other' originated from Saudi Arabia and Jordan. The depth that MN penetrated to in skin did not remain constant throughout the study period in all participants, yet the fluctuations did not show any distinct trend (Figure 3A). A significant difference in the mean penetration depths measured at t = 0 was found between males and females, with an increased penetration depth associated with volunteers who were male ($p = 0.002$). This was unexpected, not being readily explainable, and differs from other volunteer studies we have conducted[13], possibly due to the relatively small numbers here. However, for all other time points, no significant difference in penetration depth was observed, nor was there any difference between the volunteers at each of the time points investigated. Critically, MN did not retract from skin, even after 6 hours' insertion.

### Microneedles in skin

The mean initial mass of MN arrays was 26.4 ± 1.1 mg (n = 45). The percentage increase in mass for MN arrays was found to increase significantly with in-skin residence time ($p < 0.001$) (Figure 3B), as the MN took up skin interstitial fluid (Figure 3C). There was no significant difference in the percentage mass increase between the volunteers. Importantly, MN patches were always removed intact from the volunteers' skin (Figure 3E). OCT scans indicated that the mean MN height and base diameter for each volunteer increased progressively with time up to 4 hours. Slight declines were noted at 6 hours, possibly due to

the Sellotape® losing adhesion somewhat, facilitating evaporation with concomitant de-swelling. However, even after 6 hours, the mean MN height was still significantly greater than at t = 0, being measured at approximately 739 ± 143 μm and the mean MN base diameter was approximately 370 ± 85 μm, which was also significantly greater than the initial base diameter ($p < 0.05$ in both cases). MN volume, calculated using their individual heights and base diameters and based on the assumption of a conical MN shape, was used to illustrate the variation in MN size with increasing MN residence time within the skin (Figure 3D).

## Transepidermal water loss (TEWL)

The mean baseline TEWL prior to MN application ranged between 5.3 (± 0.4) and 22.2 (± 3.8) g/m$^2$hr, with a median value of 9.5 (± 0.53) for the 15 volunteers. Males had significantly greater baseline TEWL values ($p < 0.001$) when compared with females. However, this may again be distorted by the relatively small volunteer numbers here, since there are no known sex-dependent differences in mean TEWL values. Immediately following patch removal, a significant increase from the baseline TEWL (g/m$^2$hr) measured before patch application was observed for all patch residence times. The change in TEWL at removal (t = 0) was not found to be significantly different between the MN-free patch and the 0.5 hour MN patch, possibly due to the effect of occlusion by the MN-free patch. The smallest change in TEWL (relative to baseline) immediately following patch removal (t = 0) was associated with the MN-free patch, for which a mean TEWL value of 7.8 (± 3.0) g/m$^2$hr was recorded. For the MN-containing patches, the change in TEWL increased progressively as the duration of MN patch residence increased, with the greatest overall change in TEWL measured at 19.2 (± 7.2) g/m$^2$hr for the 6 hour MN patch at t = 0. The mean % change in TEWL for the various scenarios are presented in Figure 4A. The differences between MN treated skin and that treated with the “placebo” MN-free patch are very clear, thus illustrating the influence of MN on skin barrier function and its recovery, as distinct from simple occlusion.

The most prompt recovery of skin barrier function for MN treated skin, as evidenced by a return to baseline TEWL values, was seen for the MN-free patch, followed by the shortest MN patch residence time of 0.5 hours. Importantly, TEWL at 24 hours, while variable, was not significantly different from baseline, regardless of the duration of MN residence in skin ($p > 0.05$ in all cases).

## Optical coherence tomography (OCT)

OCT was used to measure the depth and width of MN-created micropores in 8 volunteers (F5, F6, F7, M4, M5, M6, M7 and M8) over time post MN removal. OCT scans were converted to the aerial perspective (Figure 4B) and then transposed back to the 2d side-on-view for measurement (Figure 4C). In all cases, micropores were still visible using OCT 24 hours after MN patch removal, suggesting that skin recovery was not complete at this time point, even though TEWL values had returned to baseline.

### Measurements of sensation and skin appearance

The measures of sensation experienced during MN insertion, during MN patch wear for 6 hours and MN-free patch wear for 6 hours obtained using the SF-MPQ are summarised in Table 2A. In all three stages of pain assessment, the PRI descriptors were rated as none or mild and the total and sensory PRI scores were equivalent, i.e. no affective descriptors identified. Although no statistically significant difference was found between the PRI scores for MN insertion and during the 6 hours of MN patch wear, the descriptors rated as 'mild' which were unique to MN insertion were 'shooting', 'stabbing' and 'heavy'. The mean PRI score for the 6 hour duration of wear for the MN-free patch also showed no significant difference to the MN-containing patch. In contrast to the MN patch, however, mild 'aching' was not experienced for the MN-free patch wear. For all instances of pain measurement, the maximum PPI (2.0) was associated with MN insertion and the maximum VAS (2.1) was actually relating to the MN-free patch wear, as shown in Table 2A. Any differences in PPI and VAS scores, however, were not found to be significant ($p = 0.05$).

Minor erythema was visible in all volunteers following the removal of MN patches, as shown in Table 2B, although this was not specifically measured. This erythema was usually associated with the area of direct contact with the MN, rather than from the area in contact with the Sellotape®. Erythema appeared to reduce with MN residence time, indicating that it may be the process of initial insertion that is the cause. Since our MN are made from biocompatible materials that become soft upon swelling in skin, they will not cause ongoing skin damage or mechanical irritation like a hard metal or silicon MN system could. Accordingly, recovery is likely to progress during MN residence with our system. In the majority of volunteers, any erythema present had disappeared completely within a few hours of removal, but for a few was more prolonged, resolving after 48 hours. There was no evidence of local skin reactions or infections when volunteers were followed up at weekly intervals for 4 weeks.

### Volunteer feedback

One third of volunteers stated on the questionnaire that they noticed a "difference" between patch applications at different locations, but only 20% of the participants overall detailed the area relating to the MN-free patch to have been less painful. Only 6 of the 15 participants provided additional commentary. The comments relating to MN insertion were focussed on the force used for manual application.

> *'You just feel pressure on your arm.'* (F1)

> *'Any discomfort felt was probably down to the manual pressing on of the microneedles rather than penetration of the microneedles themselves.'* (M2)

Most comments related to the discomfort experienced as a result of the Sellotape® used for attachment to the skin, rather than the MN arrays. Some participants attributed the itching and irritation experienced to this mode of adhesion.

> *'Slight signs of irritation showing at edges of sellotape and itchiness…'* (M1)

> *'…a little bit of itching. Don't know whether the microneedles or the sellotape.'* (F1)

Additionally, some male volunteers only commented on discomfort associated with the stripping of arm hair during patch removal.

> *'The only discomfort during the experiment was from the tape pulling my arm hairs, not from the needles.'* (M2)
>
> *'Better to shave prior…'* (M1)

## Discussion

The unique formulation of our hydrogel-forming MN means that they take up skin interstitial fluid upon insertion and swell, with the degree of polymer crosslinking controlling the swelling which, in turn, controls drug release. Accordingly, such MN act initially as a tool to penetrate the *stratum corneum* barrier. Upon swelling, they become a rate controlling membrane. While we have extensively investigated drug delivery using these unique MN systems both *in vitro* and *in vivo* in animals models[10,12], we have never before quantified fluid uptake or skin barrier recovery in human volunteers.

The estimated fluid uptake range in one hour of 0.9 - 2.7 μl (assuming a fluid density of 1 mg/ml) found for the MN here was of the same order of magnitude as the rates of interstitial fluid uptake for hollow MN, microdialysis and a technique involving a low energy laser for pore creation and a vacuum for fluid extraction.[22,23,24] Accordingly, assuming drug substances can be extracted from the swollen MN post-removal from skin, and knowing that skin interstitial fluid concentrations of drug substances often reflect those in blood plasma[25], our hydrogel-forming MN may prove useful in minimally-invasive patient monitoring as well as in drug/vaccine delivery.

OCT confirmed that the MN swelled in the volunteers' skin during residence. However, in a number of cases (10 volunteers), a drop in mean MN volume was observed between the 4 hour and 6 hour time points. It is possible that the reduced performance of the Sellotape® after the 4 hour time point allows evaporation and de-swelling of the MN. Furthermore, the slight discomfort and irritation identified by some as a result of the Sellotape® may have encouraged greater subconscious patch interference by the volunteers, further compromising adhesion. It should be noted that Sellotape® was not selected as an ideal adhesive backing in this respect and, rather, was employed to facilitate the *in situ* OCT imaging of the MN due to its transparency. However, the discomfort experienced does highlight the importance of careful adhesive selection for MN patch design. Clearly, there is a need to ensure comfort and non-irritancy, but also to ensure the swelling process is not compromised in any way. While flexibility is important to facilitate swelling, optimum security is important to prevent MN retraction from the skin. Crucially, MN did not retract from skin here and were removed fully intact in all cases. This is in agreement with our previous work with such MN.[10,11,14] While OCT indicated differences in penetration depth at t = 0, there was little difference in penetration depth beyond this time point, once the swelling process had begun. This may suggest penetration depth to be of limited consequence when using hydrogel-forming MN arrays, thus reducing concerns regarding the consistency of depth penetration of MN when applied by hand. Such manual application will be more convenient, especially for patient self-application and application to children, by removing the need for additional equipment.

The skin recovery process following MN application and removal is not well understood, but is vitally important. The skin acts as an important two-way barrier controlling the movement of water and electrolytes inward and outward, in addition to defending against microorganisms and UV radiation.[26] This study is the first to simultaneously employ TEWL and OCT as a dual approach to follow skin recovery after MN removal and demonstrates a discrepancy between the two methods. OCT indicated the presence of micropores 24 hours after MN removal in all cases, even when TEWL readings had indicated that barrier function had returned to normal. While TEWL measurements indicated a complete recovery of the area following the removal of the MN patch at the 24 hour measurement, OCT images still indicated the presence of micropores. The inconsistencies between TEWL and imaging techniques have already been highlighted.[5,27] In those previous studies, TEWL was reported to underestimate pore closure at 4-5 hours for MN with heights of 370 and 770 μm, in comparison to the greater time frame indicated by calcein dye imaging of 12 and 18 hours, respectively[5,27]. The variability associated with TEWL measurement, as a result of various volunteer and environmental factors, may represent one explanation for such discrepancies. While skin recovery has been intentionally extended to longer time points by occlusion, many previous studies indicate a complete recovery in the absence of occlusion within much shorter time frames, such as 30 minutes, as indicated by TEWL, and 2 hours, as indicated by skin impendence spectroscopy.[4,10,11,28] A more likely explanation for the inconsistencies between TEWL and OCT detected in the present study could be that the skin actually exhibited a quicker recovery than indicated by OCT and only skin indentations remained. Such circumstances could represent an important limitation of OCT, and indeed, other imaging technique in MN studies. More extensive work in the area of pore recovery following MN application is, therefore, required to increase understanding.

This study found post-removal TEWL to progressively increase as the duration of MN patch residence increased, from the 0.5 hour to 6 hour time point. Similarly, previous work employing tape stripping found that an increased contact time resulted in a greater change in TEWL.[29] Contrastingly, pore analysis using OCT failed to identify a significant difference between the different residence times. It is possible, therefore, that greater MN residence times do not in fact impact on skin recovery to any greater extent than shorter residence times and the increased TEWL values are actually caused by a separate issue, such as the longer duration of occlusion of the skin.[29] The lower change in TEWL found for the MN-free patch, in comparison to the MN patch, was not unexpected and has also been previously demonstrated.[11] Although involving only small numbers, comparisons between volunteers indicated that there was no meaningful difference in the recovery achieved during the 24 hour study period. Further work is now required to study pore closure kinetics in a large multiethnic population and in different age groups. The effect of participant characteristics, such as age, gender and skin type, as well as MN patch characteristics, such as MN geometry and patch backing layer design, should be fully examined. The pore assessments should also involve the employment of various techniques simultaneously. Furthermore, there is a need for further methodological developments within OCT technology to optimise this approach and enable more accurate measurement of key features of interest. A method involving the selection and automatic measurement of such features could improve efficiency and accuracy, compared to the current manual measurement approach.

There were no complaints of skin reactions, adverse events or strong views against MN patch use by any of the volunteers. Only some minor erythema was noted after patch removal, although this always resolved within 48 hours and no adverse events were present on follow-up. Taken together with the encouraging skin recovery data and promising fluid uptake measurements, further clinical examination of hydrogel-forming MN in both delivery and monitoring applications is clearly warranted. It is likely that approval for delivery and monitoring products based on this technology will need to be obtained from regulatory bodies on a case by case (drug by drug for delivery applications) basis. Accordingly, the influence of each drug substance to be delivered on MN performance, skin reactivity and barrier recovery will need to be extensively studied and the data included in product submission documentation. Since some MN patches for drug delivery or monitoring purposes may be applied for up to several days, the influence of long term residence on skin tolerance and barrier function recovery post-removal will also have to be investigated.

## Acknowledgments

This work was supported by the Biotechnology and Biological Sciences Research Council (BB/K020234/1) and the Wellcome Trust (WT094085MA). The authors thank Dr Daniel Woods from Michelson Diagnostics for his technical advice and assistance with image processing in the optical coherence tomography experiments.

## References

1. Donnelly, RF.; Thakur, RRS.; Morrow, DIJ.; Woolfson, AD. Microneedle-mediated Transdermal and Intradermal Drug Delivery. 1st ed. Wiley-Blackwell; Oxford:
2. Pierre MB, Rossetti FC. Microneedle-based drug delivery systems for transdermal route. Curr Drug Targets. 2013
3. Mahmood TMT, McCrudden MTC, Torrisi BM, McAlister E, Donnelly RF. Microneedles for intradermal and transdermal delivery. Eur J Pharm Sci. 2013; 50:623–37. [PubMed: 23680534]
4. Li G, Badkar A, Kalluri H, Banga AK. Microchannels created by sugar and metal microneedles: characterization by microscopy, macromolecular flux and other techniques. J Pharm Sci. 2010; 4:1931–41. [PubMed: 19894263]
5. Kalluri H, Kolli CS, Banga AK. Characterization of microchannels created by metal microneedles: formation and closure. AAPS J. 2011; 3:473–81. [PubMed: 21732220]
6. Ghosh P, Brogden NK, Stinchcomb AL. Fluvastatin as a Micropore Lifetime Enhancer for Sustained Delivery Across Microneedle-Treated Skin. J Pharm Sci. 2014 doi: 10.1002/jps.23844.
7. Brogden NK, Banks SL, Crofford LJ, Stinchcomb AL. Diclofenac enables unprecedented week-long microneedle-enhanced delivery of a skin impermeable medication in humans. Pharm Res. 2013; 30:1947–55. [PubMed: 23761054]
8. Brogden NK, Milewski M, Ghosh P, Hardi L, Crofford LJ, Stinchcomb AL. Diclofenac delays micropore closure following microneedle treatment in human subjects. J Control Release. 2012; 163:220–9. [PubMed: 22929967]
9. Ghosh P, Brogden NK, Stinchcomb AL. Effect of formulation pH on transport of naltrexone species and pore closure in microneedle-enhanced transdermal drug delivery. Mol Pharm. 2013; 10:2331–9. [PubMed: 23590208]
10. Donnelly RF, Thakur RRS, Garland MJ, Migalska K, Majithiya R, McCrudden CM. Hydrogel-forming microneedle arrays for enhanced transdermal drug delivery. Adv Funct Mat. 2012; 22:4879–4890.
11. Donnelly RF, Thakur RRS, McCrudden MTC, Zaid-Alkilani A, O'Mahony C, Armstrong K, McLoone N, Kole P, Woolfson AD. Hydrogel-forming microneedle arrays exhibit antimicrobial properties: Potential for enhanced patient safety. Int J Pharm. 2013; 451:76–91. [PubMed: 23644043]

12. Donnelly RF, Morrow DIJ, McCrudden MTC, Zaid-Alkilani A, Vicente-Perez EM, O'Mahony C, González-Vázquez P, McCarron PA, Woolfson AD. Hydrogel-forming and dissolving microneedles for enhanced delivery of photosensitisers and precursors. Photochem Photobiol. 2014 doi: 10.1111/php.12209.
13. Donnelly RF, Moffatt K, Zaid-Alkilani A, Vicente-Perez EM, Barry J, McCrudden MTC, Woolfson AD. Hydrogel-forming microneedle arrays can be effectively inserted in skin by self-application: A pilot study centred on pharmacist intervention and a patient information leaflet. Pharm Res. 2014 In Press.
14. Thakur RRS, McCarron PA, Woolfson AD, Donnelly RF. Investigation of swelling and network parameters of poly (ethylene glycol)-crosslinked poly (methyl vinyl ether-*co*-maleic acid) hydrogels. Eur Polym J. 2009; 45:1239–1249.
15. McCarron PA, Woolfson AD, Donnelly RF, Andrews GP, Zawislak A, Price JH. Influence of Plasticiser Type and Storage Conditions on the Properties of Poly(methyl vinyl ether-*co*-maleic anhydride) Bioadhesive Films. J Appl Polym Sci. 2004; 91:1576–1589.
16. Pinnagoda J, Tupker RA, Agner T, Serup J. "Guidelines for transepidermal water loss (TEWL) measurement. A report from the Standardization Group of the European Society of Contact Dermatitis.", Guidelines for transepidermal water loss (TEWL) measurement. A report from the Standardization Group of the European Society of Contact Dermatitis. 1999; 22:164–78.
17. Mogensen M, Thrane L, Joergensen TM, Anderson PE, Jemec GBE. Optical coherence tomography for imaging of skin and skin diseases. Semin Cutan Med Surg. 2009; 28:196–202. [PubMed: 19782944]
18. Fercher AF. Optical Coherence Tomography – development, principles, applications. Z Med Phys. 2010; 20:251–276. [PubMed: 21134630]
19. Donnelly RF, Garland MJ, Morrow DIJ, Migalska K, Thakur RRS, Majithiya R. Optical coherence tomography is a valuable tool in the study of the effects of microneedle geometry on skin penetration characteristics and in-skin dissolution. J Cont Rel. 2010; 147:333–341.
20. Donnelly RF, Majithiya R, Thakur RRS, Morrow DIJ, Garland MJ, Demir YK. Design and physicochemical characterisation of optimised polymeric microneedle arrays prepared by a novel laser-based micromoulding technique. Pharm Res. 2011; 28:41–57. [PubMed: 20490627]
21. Burckhardt CS, Jones KD. Adult measures of pain: The McGill Pain Questionnaire (MPQ), Rheumatoid Arthritis Pain Scale (RAPS), Short-Form McGill Pain Questionnaire (SF-MPQ), Verbal Descriptive Scale (VDS), Visual Analog Scale (VAS), and West Haven-Yale Multidisciplinary Pain Inventory (WHYMPI). Arthrit Care Res. 2003; 49:96–104.
22. Gardeniers H, Luttge R, Berenschot E, de Boer M, Yeshurun S. Silicon micromachined hollow microneedles for transdermal liquid transport. J Microelectromech. 2003; 12:855–862.
23. Sun H, Bungay PM, Elmquist WF. Effect of Capillary Efflux Transport Inhibition on the Determination of Probe Recovery During in Vivo Microdialysis in the Brain. J Pharmcol Exp Ther. 2001; 297:91–100.
24. Venugopal M, Feuvrel K, Mongin D, Bambot S, Faupel M, Panangadan A. Clinical evaluation of a novel interstitial fluid sensor system for remote continuous alcohol monitoring. IEEE Sensors J. 2008; 8:71–80.
25. Delgado-Charro M, Guy R. Transdermal reverse iontophoresis of valproate: A noninvasive method for therapeutic drug monitoring. Pharm Res. 2003; 20:1508–1513. [PubMed: 14567648]
26. Burns, DA.; Rook, AJ. Rook's Textbook of dermatology. 8th ed. Wiley-Blackwell; Oxford: 2010.
27. Kalluri H, Banga A. Formation and Closure of Microchannels in Skin Following Microporation. Pharm res. 2011; 28:82–94. [PubMed: 20354766]
28. Gupta J, Gill H, Andrews S, Prausnitz M. Kinetics of skin resealing after insertion of microneedles in human subjects. J Control Release. 2011; 154:148–55. [PubMed: 21640148]
29. Loffler H, Dreher F, Maibach HI. Stratum corneum adhesive tape stripping: influence of anatomical site, application pressure, duration and removal. Brit J Dermatol. 2004; 151:746–752. [PubMed: 15491413]

Europe PMC Funders Author Manuscripts

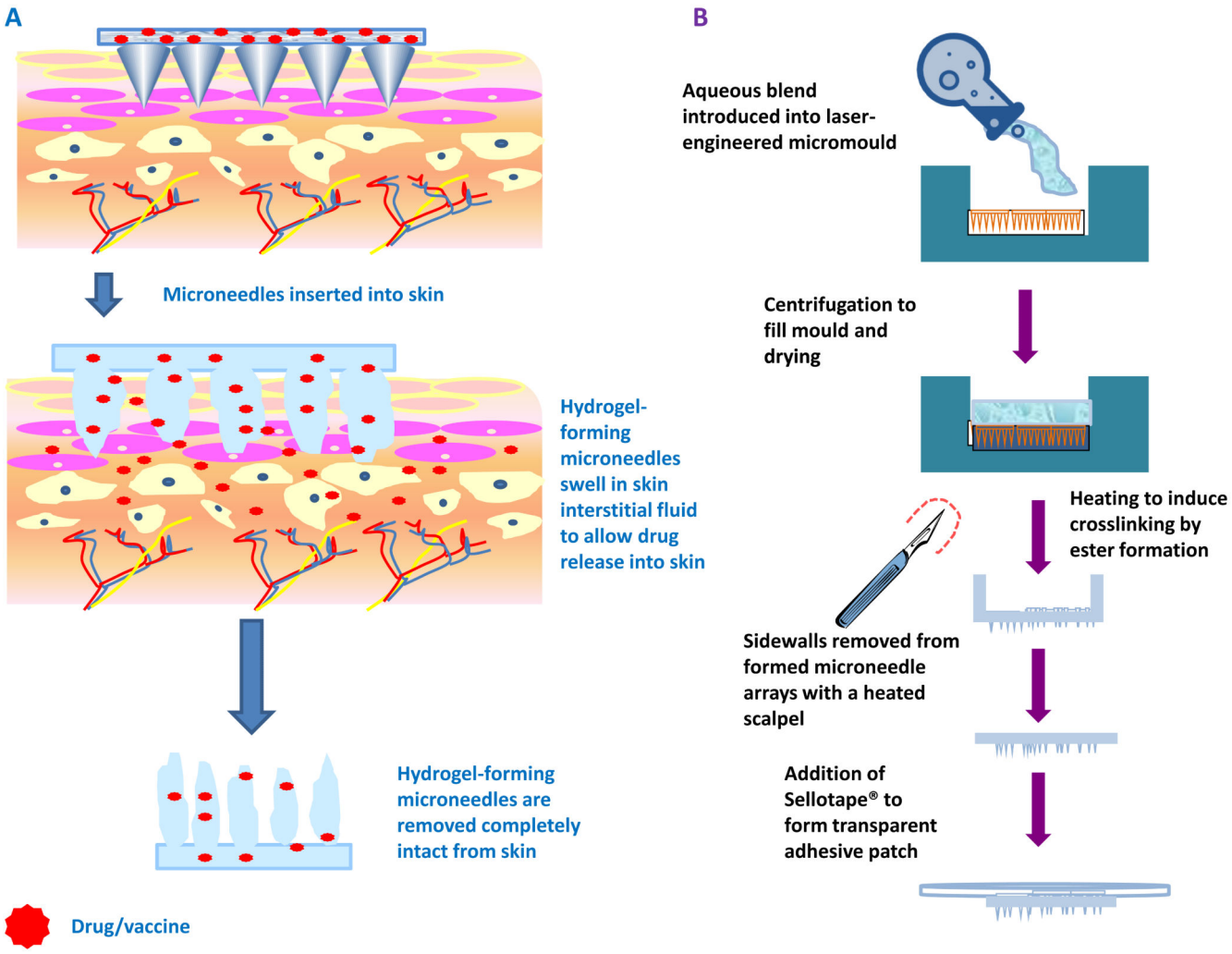


**Figure 1.**

Schematic illustration of the mechanism of drug delivery from hydrogel-forming microneedle arrays with attached patch-type drug reservoirs **(A)**.

Schematic representation of casting and crosslinking of hydrogel-forming microneedle arrays and addition of Sellotape® to form a transparent adhesive patch **(B)**.

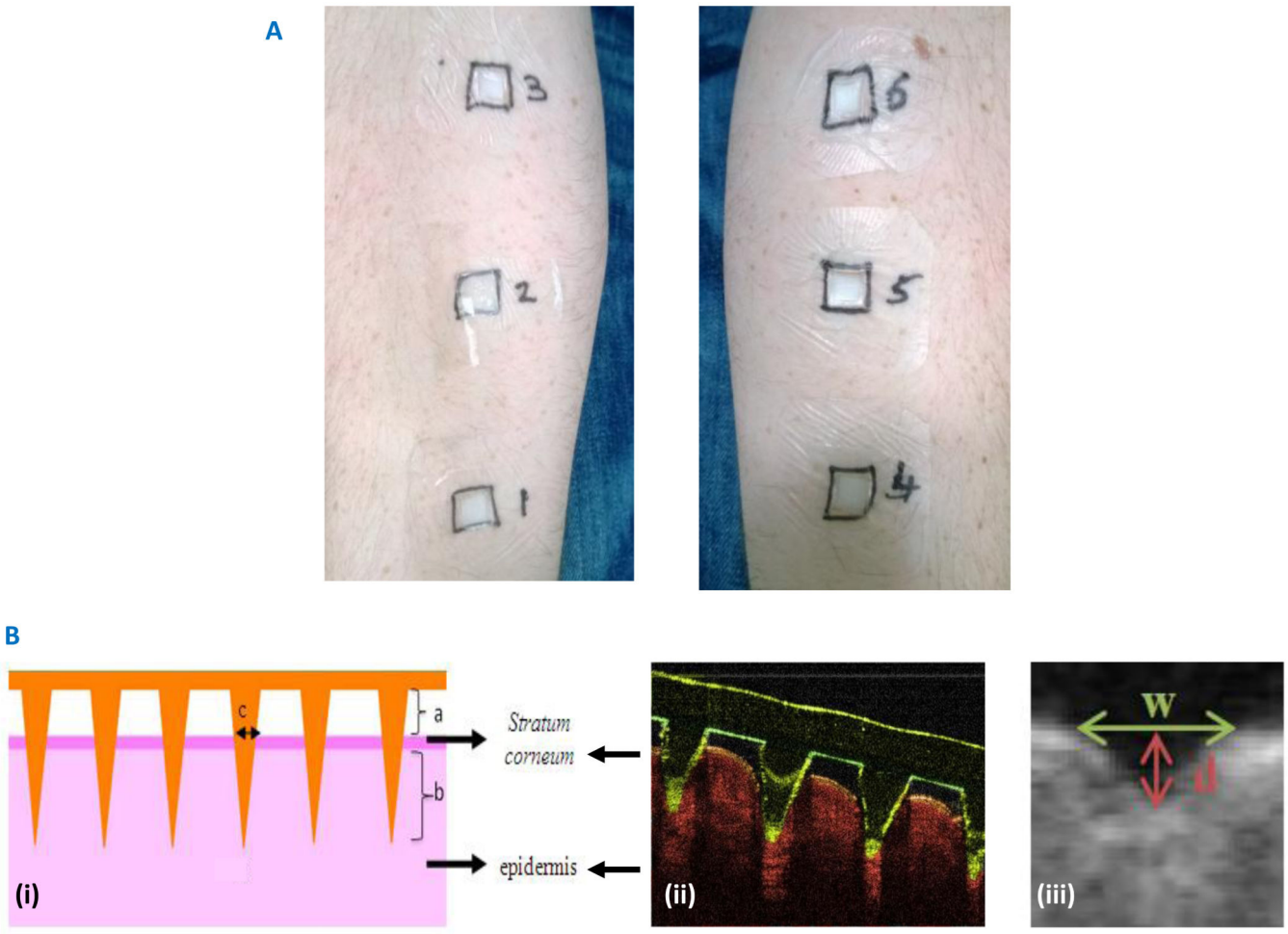


**Figure 2.**

Representative patch application on the ventral forearm of human volunteers **(A)** **(B)** Panel **(i)** shows a diagrammatic representation of the measurements that are possible from the optical coherence tomographic images of microneedle penetration into volunteers' skin *in vitro*, namely; (a) the distance between the lower microneedle base plate and the *stratum corneum*, (b) the depth of microneedle penetration into the skin and (c) the width of the micropore created in the skin.

Panel **(ii)** shows a representative cross sectional optical coherence tomographic image, with false colours applied.

Panel **(iii)** shows a representative pore after microneedle removal with the measurements taken clearly outlined (d depth, w width).




Europe PMC Funders Author Manuscripts

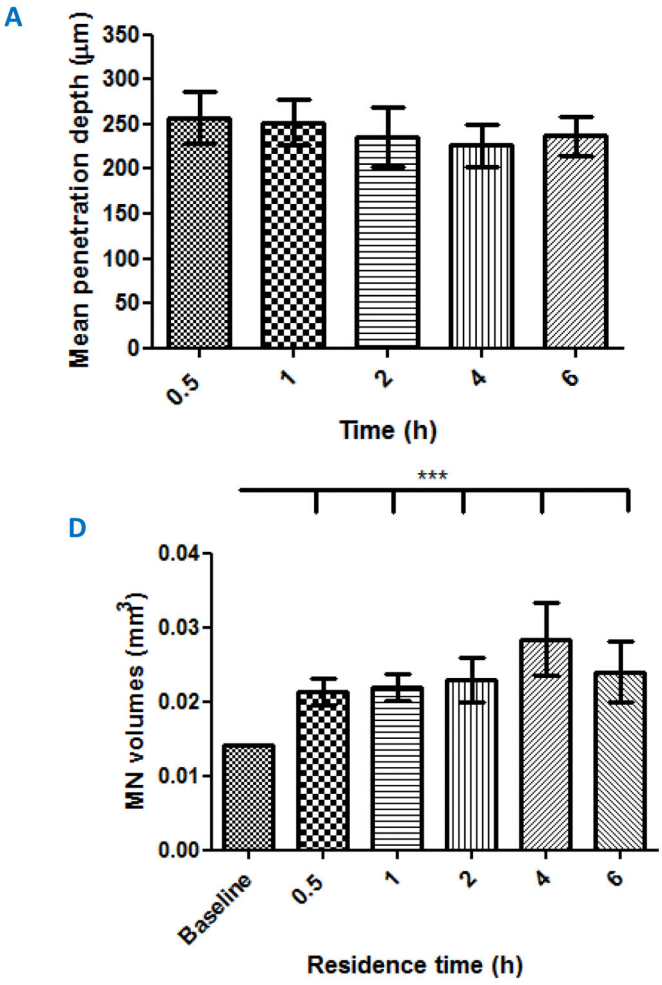


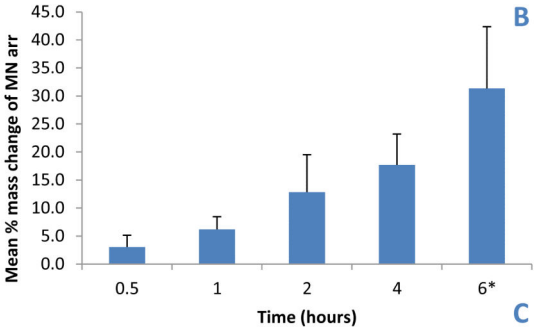


C

| MN residence time (hours) | Estimated fluid uptake (mg) | |
|---|---|---|
| | Mean (± S.D.) | Range |
| **0.5** | 0.76 (± 0.46) | 0.2 - 2.7 |
| **1** | 1.63 (± 0.58) | 0.9 - 2.7 |
| **2** | 3.11 (± 1.57) | 1.0 - 6.5 |
| **4** | 4.98 (± 1.83) | 1.8 - 8.5 |
| **6*** | 8.38 (± 3.03) | 3 - 12.3 |

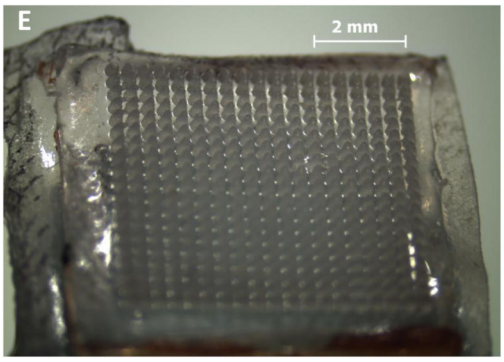


**Figure 3.**

Variation in mean (± S.D.) penetration depth of microneedles (n = 36 measurements of depth) in the 15 volunteers' skin with residence time **(A)**.

Mean (± S.D.) % mass change (n = 15) of the microneedle arrays after various residence times within the skin of the volunteers (* n = 13 at 6 hours) **(B)**.

Estimated fluid uptake per microneedle array (n = 15) following removal from the skin after various residence times **(C)**.

Variation in mean (± S.D.) volume of microneedles (n = 36) with different microneedle residence times for the 15 volunteers based on the estimated microneedle height and base diameter measurements obtained from optical coherence tomography scans and assuming the area of a cone compared to the estimated volume at t = 0 **(D)**.

Typical morphology of a hydrogel-forming microneedle arrays post-removal for the longest residence time of 6 hours **(E)**.

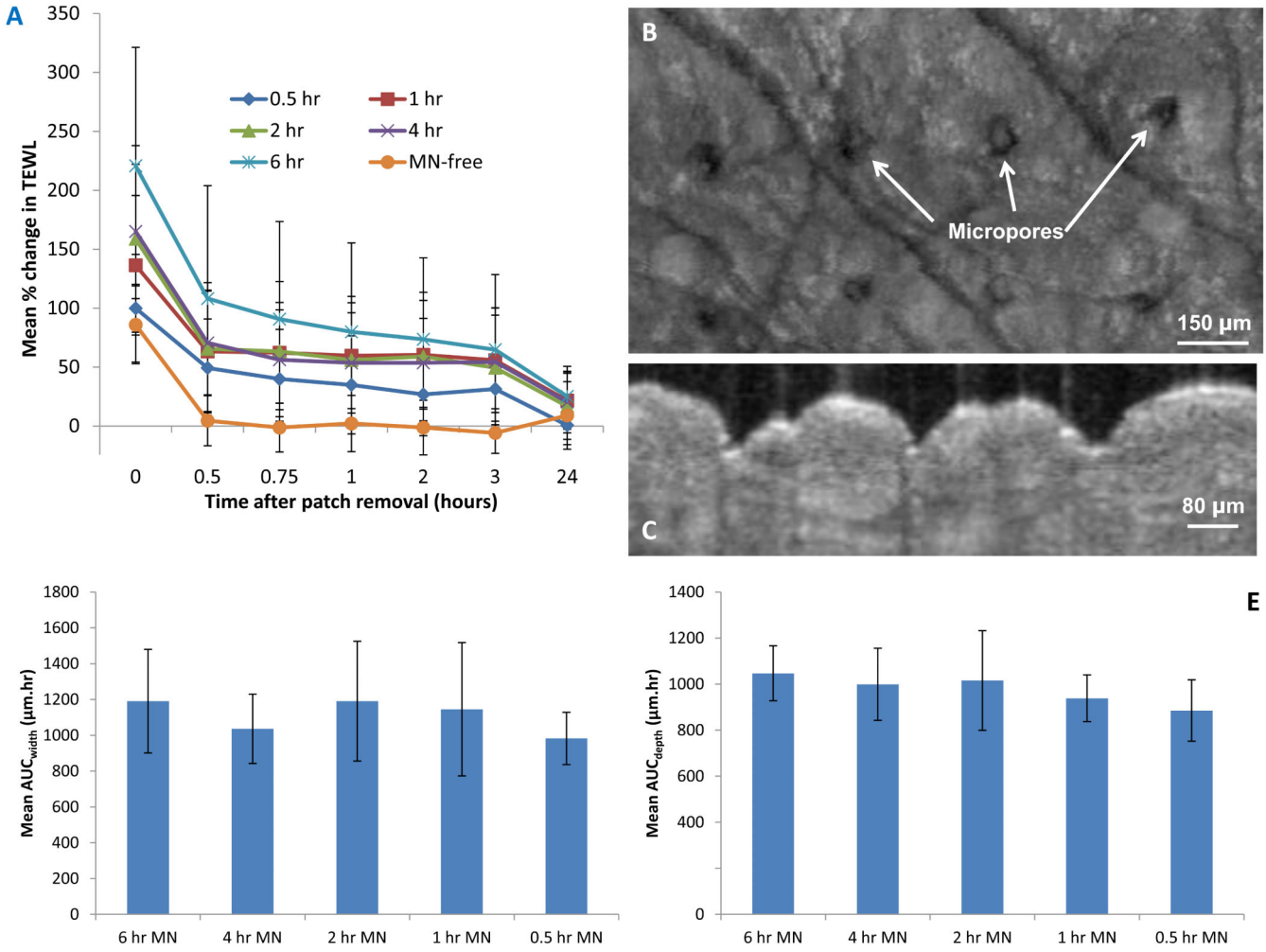


**Figure 4.**

Mean % change (+ S.D.) in transepidermal water loss (n = 15) over time for the for the 6 different modes of microneedle and baseplate patch application **(A)**.

Representative optical coherence tomography image of the skin (aerial perspective) with visible line of micropores 24 hours after removal of a microneedle patch applied to the skin for a 6 hour time period **(B)**.

Representative optical coherence tomography image of the skin taken immediately after microneedle removal following a 6 hour residence time after conversion to the 2d side-on view **(C)**.

Mean (± S.D.) area under curve (AUC) (n = 8) values for the plot pore depth (µm) against time, i.e. $AUC_{depth}$, as measured from optical coherence tomography scans of the skin following the removal of microneedle patches following the various durations of microneedle skin residence **(D)**.

Mean (± S.D.) AUC (n = 8) for the plot pore width against time, i.e. $AUC_{width}$, as measured from OCT scans of the skin following the removal of MN patches following the various durations of microneedle skin residence **(E)**.

**Table 1**

Type and duration of patch application for each application site (A).
Occasions of the administration of the SF-MPQ (B).
The demographic information for the human volunteers (C).

A

| Application Site | Residence time / hr | Patch type |
|---|---|---|
| **1** | 6 | MN |
| **2** | 6 | MN-free |
| **3** | 4 | MN |
| **4** | 2 | MN |
| **5** | 1 | MN |
| **6** | 0.5 | MN |

B

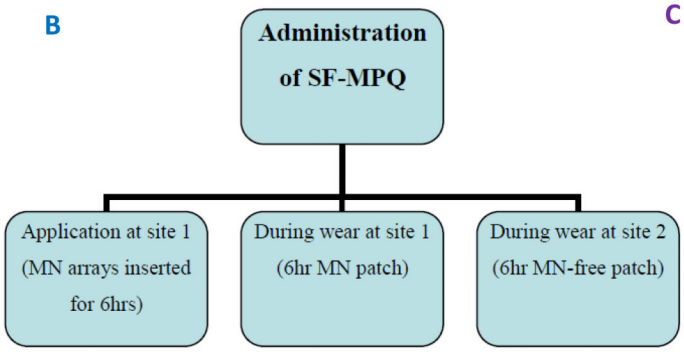


C

| Volunteer ID | Gender | Age | Ethnicity |
|---|---|---|---|
| **M1** | Male | 35 | White other |
| **F1** | Female | 25 | White other |
| **F2** | Female | 30 | Other |
| **M2** | Male | 31 | White Irish |
| **F3** | Female | 28 | Other |
| **F4** | Female | 53 | White/Black Caribbean |
| **M3** | Male | 24 | White British |
| **F5** | Female | 25 | White British |
| **F6** | Female | 25 | White British |
| **F7** | Female | 25 | White British |
| **M4** | Male | 28 | Indian |
| **M5** | Male | 33 | Other Asian |
| **M6** | Male | 24 | White British |
| **M7** | Male | 35 | White other |
| **M8** | Male | 28 | White British |

## Table 2

Summary of pain scores obtained by administration of the SF-MPQ (n = 15) for three instances: Microneedle insertion; during the 6 hour period of microneedle patch wear; and, during the 6 hour period of microneedle-free (baseplate only) patch wear (A).

Representative digital photographs of volunteers' skin prior to, and post microneedle removal (B).

**A**

| SF-MPQ | | Patch wear | |
|---|---|---|---|
| | | MN | MN-free |
| Mean (+/-SD) Pain Rating Index (PRI) *(range)* | 1.2 (+/- 1.26) *(0 – 4.0)* | 0.53 (+/- 0.92) *(0 – 3.0)* | 0.27 (+/- 0.59) *(0 – 2.0)* |
| Mean (+/-SD) Visual Analogue Scale (VAS) *(range)* | 0.65 (+/- 0.58) *(0 – 1.9)* | 0.28 (+/- 0.31) *(0 – 0.95)* | 0.38 (+/- 0.64) *(0 – 2.1)* |
| Mean (+/-SD) Present Pain Intensity (PPI) *(range)* | 0.66 (+/- 0.82) *(0 – 2.0)* | 0.2 (+/- 0.41) *(0 – 1.0)* | 0.13 (+/- 0.35) *(0 – 1.0)* |

**B**

| Application site | Patch type | Residence time (h) | Prior to application | Immediately following removal | 2 h post-removal | 24 h post-removal |
|---|---|---|---|---|---|---|
| 6 | MN | 0.5 | 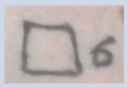 |  |  |  |
| 5 | MN | 1 | 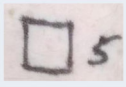 |  |  |  |
| 4 | MN | 2 | 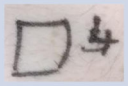 | 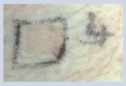 |  |  |
| 3 | MN | 4 | 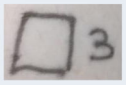 |  |  |  |
| 2 | MN-free | 6 | 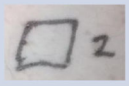 |  |  |  |
| 1 | MN | 6 |  |  |  |  |